Advanced Composite Materials
Publication details, including instructions for authors and subscription information:
http://www.tandfonline.com/loi/tacm20

Experiments and numerical analysis of compression after impact (CAI) behavior of CF/PIXA stiffened panels for HSCT structure

Takashi Ishikawa , Masamichi Matsushima , Yoichi Hayashi & Murray L. Scott

Version of record first published: 02 Apr 2012.

To cite this article: Takashi Ishikawa , Masamichi Matsushima , Yoichi Hayashi & Murray L. Scott (2005): Experiments and numerical analysis of compression after impact (CAI) behavior of CF/PIXA stiffened panels for HSCT structure, Advanced Composite Materials, 14:3, 239-261

To link to this article: http://dx.doi.org/10.1163/1568551054922638

Adv. Composite Mater., Vol. 14, No. 3, pp. 239–261 (2005)

Also available online - www.vsppub.com

Experiments and numerical analysis of compression after impact (CAI) behavior of CF/PIXA stiffened panels for HSCT structure

TAKASHI ISHIKAWA [1,*], MASAMICHI MATSUSHIMA [1], YOICHI HAYASHI [1] and MURRAY L. SCOTT [2]

[1] *Advanced Composites Evaluation Technology Center, Japan Aerospace Exploration Agency, 6-13-1 Ohsawa, Mitaka, Tokyo 181-0065, Japan*
[2] *Department of Aerospace Engineering, Royal Melbourne Institute of Technology, GPO Box 2476, Melbourne, Victoria, 3001, Australia*

Received 30 July 2004; accepted 10 December 2004

Abstract—Compression after impact (CAI) behavior of stiffened panels using T-shaped stringers made of heat resistant thermoplastic composites, CF/PIXA, was obtained by tests at room temperature and 180°C. Excellent impact resistance in terms of delamination area was verified for the present composite panels due to the special fusion bonding film. Room temperature CAI strengths of the stiffened panels were found to be better than CF/PEEK panels in a rough comparison, without regard to differences in stacking sequence and geometry. Relationships between temperature and CAI strengths for CF/PIXA stiffened panels were compared with the results for flat plates (SACMA) and a compatibility between flat plate and stiffened panel data was observed. It is clarified that damage tolerance properties of CF/PIXA stiffened structure are so remarkable at room temperature that compression strengths are quite insensitive to relative impact energy. Its damage tolerance capability is also excellent at high temperature for High Speed Civil Transport structures. Linear and nonlinear buckling analyses based on simple models without delamination and interlaminar stresses were conducted using a finite element code. The results agreed well basically with experimental results. In the case of prediction of the final strength, several points of improvement are identified. The present prediction provides the initial step to discuss the possibility of post-buckling strength design at high temperature stiffened panels.

Keywords: Heat resistant thermoplastic composites; fusion bonding; delamination resistance; ultrasonic C-scan; buckling; final failure; nonlinear finite element analysis.

*To whom correspondence should be addressed. E-mail: isikawa@chofu.jaxa.jp

1. INTRODUCTION

Weight reduction by the use of composite materials is one the most important technical issues governing feasibility of commercially promising High Speed Civil Transport (HSCT). Key requirements for such composites are thermal stability for long time duration at elevated temperature up to 177°C and excellent damage tolerance property to allow sufficient design critical strength values for light-weight structures. One promising candidate composite material is carbon fiber (IM-7 or other intermediate modulus fiber)/PIXA system. PIXA is a new high-temperature thermoplastic polyimide resin developed in Japan [1] (by Mitsui Chemicals Co. Ltd.) and it comprises a family of similar resins. The major critical strengths as composite coupon levels were evaluated at room and elevated temperatures up to 230°C previously [2, 3] by the authors including compression strength after impact (CAI) using SACMA method at 6.7 J/mm impact energy, and open hole compression (OHC) of quasi-isotropic laminates with 38.1 mm width and 6.35 mm diameter. Long-term exposure tests at high temperature air followed by the same size OHC tests as above have been being conducted [4] for one family of resin composites by another group in NAL, Japan. These basic tests demonstrated the great potential of this composite system for HSCT structure.

After acquisition of such coupon level strength data, the first step to the structure level damage tolerance evaluation was required at room and elevated temperatures. CAI tests of stiffened panels with T-shaped stringers fabricated by fusion bonding technique with special bonding film were chosen as the best compromise between desired property data and testing costs. The present paper will discuss such structural CAI properties in the light of experimental behavior and a comparison of experiments with numerical predictions using FEA. The global goal in this research program is to establish strength design criteria for the horizontal stabilizer of HSCT. Local aims in this paper are to demonstrate excellent damage tolerant properties of the present stiffened panels and to determine test allowable values for a long-term fatigue test of a model box of the same material under simulated temperature change. Subsidiary purposes are to establish experimental techniques of structural CAI tests at elevated temperature and to examine predictability of postbuckling strength of stiffened panels.

2. DESCRIPTION OF TESTED MATERIAL AND BASIC STRENGTHS

Among several heat resistant thermoplastic (HRTP) resins known to us, the family of PIX based on AURUM® polyimide resin have been developed in Japan [1]. Four types, in chronological order, PIX, PIXA, PI-SP and PIXA-M are developed and available in the marketplace. Several properties of neat resin are listed in Table 1. Material systems selected in the NAL HRTP structure research project were first IM-7/PIXA and recently IM-600/PIXA-M in accordance with a balance of material properties and availability. The present test articles are all made of IM-7/PIXA. Thus, a simpler expression of CF/PIXA will be used from here on.

Table 1.
Neat resin properties of PIX family

	PIX	PIXA	PI-SP	PIXA-M
Crystallinity (:Crs.)	Crs.	Semi-Crs.	Non-Crs.	Non-Crs.
Glass transition temperature (°C)	249	252	254	235
Tensile modulus (GPa)	2.75	2.84	2.65	—
Tensile strength (MPa)	92.2	89.2	91.2	83.4

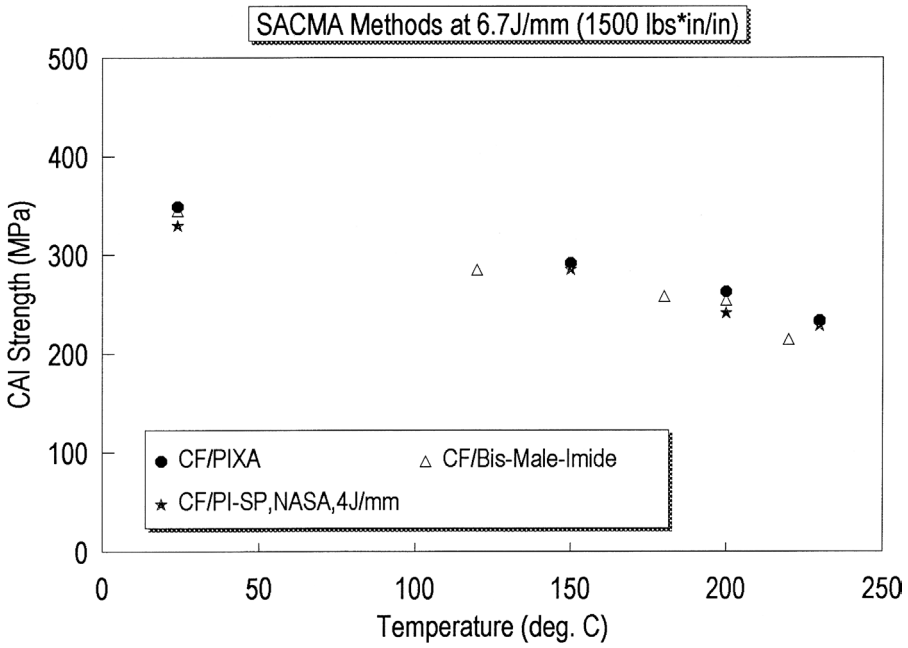

Figure 1. Comparison of flat plate CAI strengths for several high-temperature polymer composites under elevated temperature.

A brief discussion of coupon level strengths tests is given here. Open hole compression tests (OHC: $38 \times 118.0 \times 4.0^{t}$, and 6.35^{D}), no hole compression tests (NHC: $25.4 \times 105.4 \times 4.0^{t}$), and CAI tests in SACMA [5] method at 6.7 J/mm [= 1500 lbf × in/in] impact were conducted for 32 ply quasi-isotropic laminate of $\{(45/0/-45/90)^{4}/\text{sym.}\}$. They were all performed at room and elevated temperatures up to 230°C. It should be noted that all dimensions quoted above are only nominal values in mm units and that the actual values were measured for all the specimens. Detailed results of these tests were reported in Ref. [2]. In order to provide a basis for comparison discussed later, the SACMA CAI results of CF/PIXA are indicated in Fig. 1 with reference data for CF/bis-male-imide (BMI) [5260] [6] where all legends indicate an average of three data. This figure describes that the present CF/PIXA system exhibits very similar or slightly higher CAI strengths

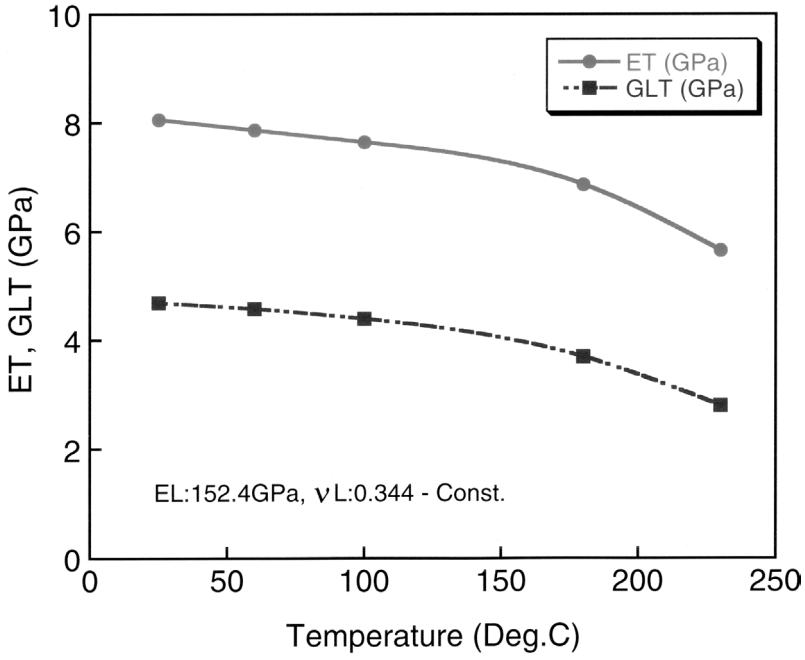

Figure 2. Temperature dependent elastic moduli (E_T and G_{LT}) of unidirectional IM-7/PIXA lamina.

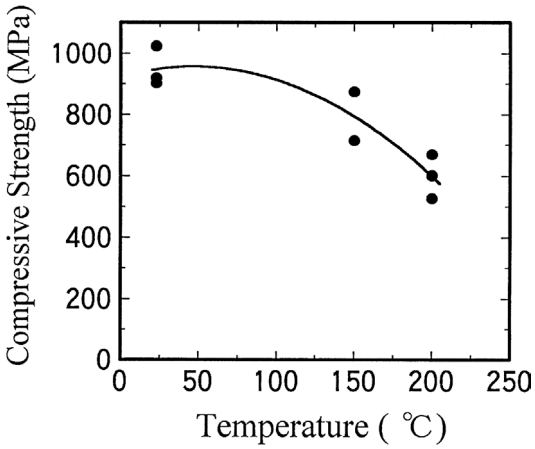

Figure 3. Temperature dependent longitudinal compressive strength data of unidirectional IM-7/PIXA by ASTM-D3410/A method.

in short term than CF/BMI. Previous CAI data [3] for similar thermoplastic PI composites (CF/PI-SP) are also plotted in Fig. 1 where the test method was NASA and normalized energy level was 4 J/mm. If we notice the energy difference between the current PIXA (6.7 J/mm) and previous PI-SP (4 J/mm) system, CAI strengths of CF/PIXA system are considered to be excellent. In this comparison, it should

be noted that a difference in CAI strengths measured by two well-known methods (NASA and SACMA) is trivial [7].

Unidirectional coupon tests were also conducted at room and elevated temperatures to determine elastic moduli and basic UD strengths. Among them, two types of results are shown in Figs 2 and 3 as input data for numerical predictions of initial buckling and strength behavior discussed later. Figure 2 shows temperature dependency of resin-controlled moduli, E_T and G_{LT}. Figure 3 indicates temperature dependent longitudinal compressive strengths of CF/PIXA UD-lamina obtained by ASTM-D3410/A method.

3. DESCRIPTION OF STIFFENED PANELS AND OUTLINE OF IMPACTS

As the first phase of damage tolerance evaluation, structural CAI strength tests were conducted for several stiffened panels of CF/PIXA with T-section stiffeners at room temperature and 180°C. The reason why this temperature was chosen is that it is slightly above a design temperature of HSCT, 177°C, although this material can endure 230°C for a medium term. For test economy, intermediate and higher temperature tests were not conducted. An outline of tested panels will be given here. Two kinds of T-stiffened panels similar to the author's previous work [8] in terms of stiffener geometry, panels with one T-stiffener (1T) and with two T-stiffeners (2T) (five panels for each kind), were fabricated by fusion bonding technique by the supporting company. Shape and dimensions of 2T and 1T panels are shown in Figs 4 and 5. In order to avoid later duplication of illustrations, strain gage and deflection pick-up locations are also indicated in these drawings as much as possible. A 2T panel has larger dimensions than 1T, although they are not necessarily sufficient in size to realize the unaffected local buckling state by peripheral supports. The size of the environmental chamber for the Instron machine used (type 1128) enforces these rather small sizes of stiffened panels. The purpose of a 1T panel is to conduct a test under less effect of local inter-bay buckling.

For fusion bonding between skin and stiffeners, a thermoplastic polyimide film, Regulus®: PIXA-M by Mitsui Chemical Co. was utilized. Panel stacking sequences were (45/90/−45/0/0/45/90/−45/0)sym.: 18 plies for skin, (45/0/−45/90/45/0/0/−45/0/0/−45/0/0/45/90/−45/0/45) sym.: 36 plies for stringer web and (45/0/−45/90/45/0/0/−45/0/0/−45/0/0/45/90/−45/0/45/45/0/−45/−45/0/45): 24 plies for stringer attachment flange. These sequences mean that the thickest portion appears at skin-stiffener bonded region of 42 plies and that it shows slight local in-plane and out-of-plane coupling effects. The stacking sequences were identical regardless of stiffener numbers.

All panels were subjected to drop weight impact tests at the one leg center of an attachment flange with energy levels of 4 J/mm and 6.7 J/mm normalized by impact location thickness. Impacts were given to the specimens at room temperature by using an instrumented drop weight machine. Delaminated area in projection was measured by an ultrasonic C-scanner, SDS 5400R system by Krautkramer

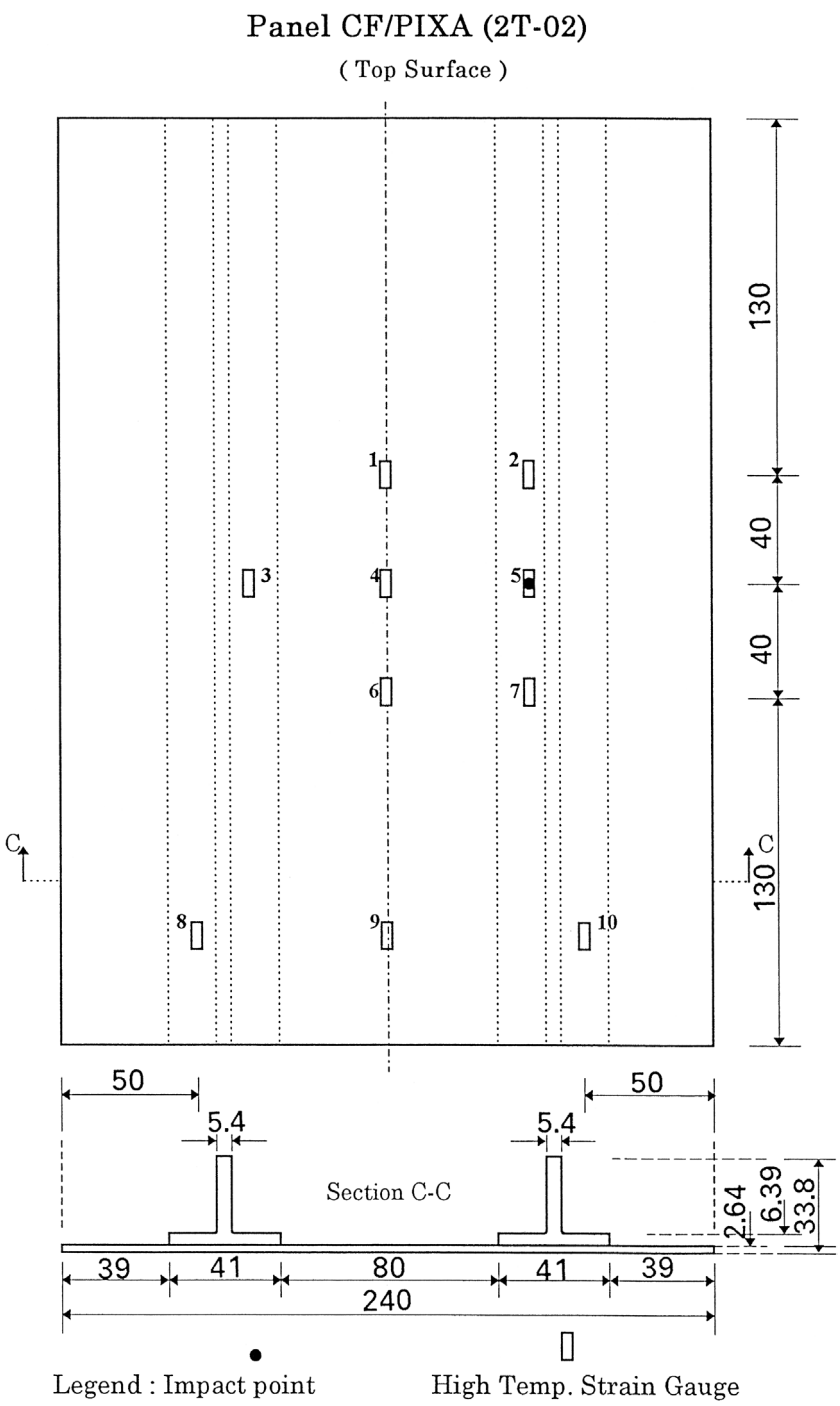

Figure 4. 2T panel geometry and locations of strain gages, deflection pick-ups and impact point.

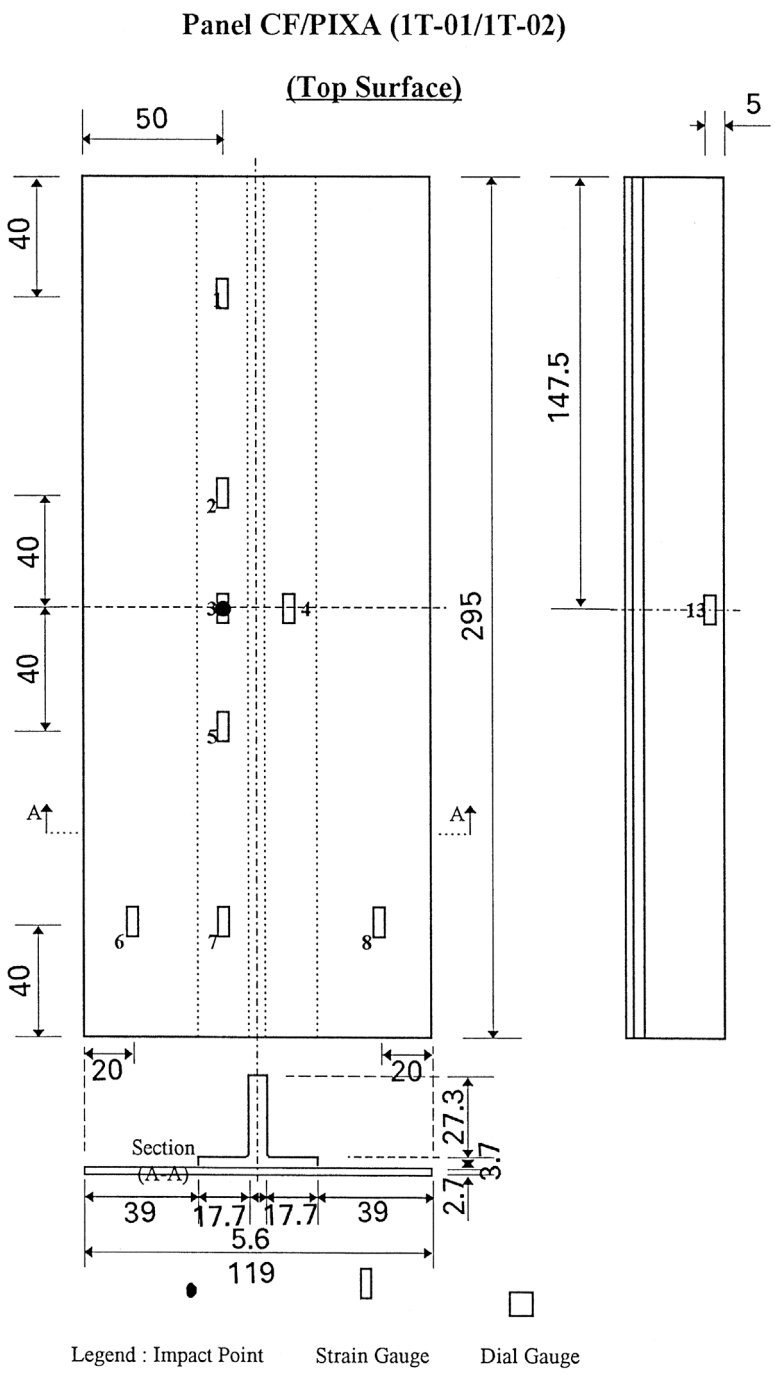

Figure 5. 1T panel geometry and locations of strain gages, deflection pick-ups and impact point.

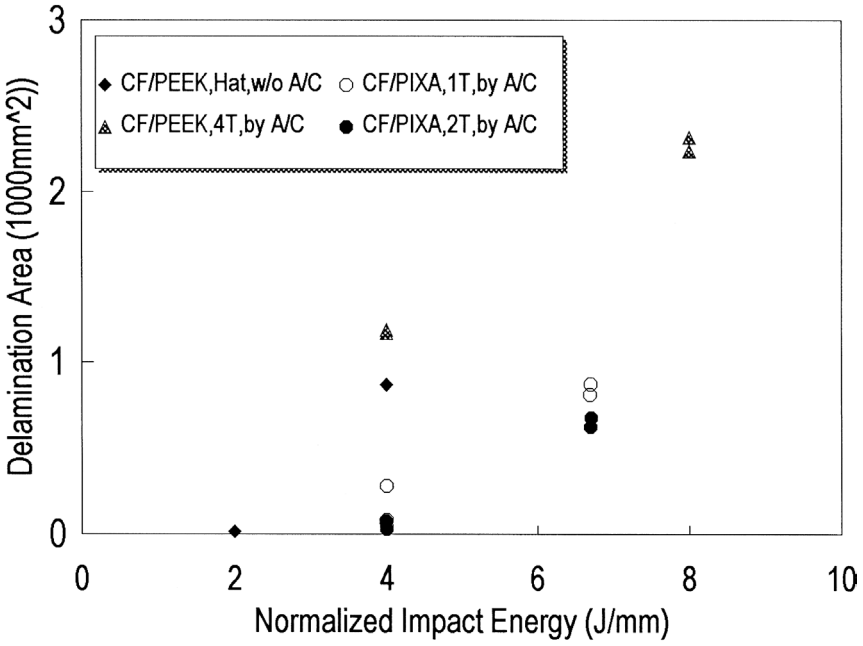

Figure 6. Relationships between normalized impact energy (energy/thickness at impact point) and projection area of delamination in CF/PIXA and CF/PEEK stiffened panels.

Japan Co. Relationships between delamination area in projection and normalized impact energy are shown in Fig. 6 for all specimens of 4 and 6.7 J/mm with the authors' previous data for CF/PEEK stiffened panels including hat-shaped stiffener types [9] for comparison. It was found that delamination areas are quite small even for 6.7 J/mm panels and that CF/PIXA has more excellent impact resistance at least at room temperature than CF/PEEK. Of course, CF/PEEK showed much higher impact resistance of CF/epoxy as described in Ref. [8]. One possible reason for this excellent impact resistance may be ascribed to the used fusion bonding film. It should be noted that this comparison in delamination area is not rigorous but qualitative if we consider a difference in panel length and average panel thickness implying a difference in energy consumption by elastic deformation during impact.

4. OUTLINE OF COMPRESSION TESTS AFTER IMPACT

Compression tests at room temperature and 180°C were conducted for 1T-01,03,04, 2T-01,05, panels, and 1T-02,05, 2T-02,03,04 panels, respectively. In room temperature tests, data acquisition devices were normal strain gages, dial gages for out-of-plane deflections, an acoustic emission sensor network system for AE location identification, and a Moiré-topography camera for obtaining out-of-plane deflection contour. Numbers of gages are 14 for 1T-01, 03, 04 and 30 for 2T-01, 05 (in channels). In elevated temperature tests, the same high temperature grade gages as flat

plate cases [2] were used with polyimide strain gage cement. The gages were only data acquisition pick-ups, except for AE measurement trials at high temperature. Gage quantities were 14 for 1T- 02, 05 and 24 for 2T-02, 03, 04. Typical gage maps are already shown in Figs 4 and 5 where some gages were glued in back-to-back locations. Gage #5 was placed on an impact indentation for 2T panels. The data logger used was a system of HP 3852A, by Hewlett–Packard Co. Ltd. Acoustic emission sensors (PAC-R15, by Physical Acoustics Co. Ltd.) for universal purpose were tried in high temperature tests and it was verified that they worked at least in 180°C atmosphere.

Intended boundary conditions were clamped along the loading and supporting edges and simply supported along two side edges. One practically difficult point in panel compression tests at high temperature is a clamping device along loading edges. Although we can rely on a potting agent [8], i.e. a mixture of epoxy resin and some filler at room temperature tests, it is very hard to find a high-temperature potting agent. Instead of potting technique, clamping fixtures of stainless steel were developed for both types of panels. A photograph of one set of the fixtures for 2T panels is shown in Fig. 7. One key element of this fixture is four wedges pressing on T-stiffener flanges activated by two main bolts. By tightening many screws for pressing rectangular pieces to the skin, clamped boundary conditions at the loading edges were approximately realized. This device was used in room temperature tests. Although there was a concern about a mismatch in coefficients of thermal expansion between CF/PIXA and stainless steel, the present experience by the authors implies that this concern is not so serious, at least at the test temperature of 180°C. A thick steel end platen (60 mm in thickness) was installed on the test machine's disc head for compression in order to give uniform displacement distribution in the loading end fixture. Stainless steel tubes with sharpened slits acting as knife-edges were installed along both side edges of the panel so that simply supported conditions were approximately realized. Compression load was applied by a screw driven machine of Instron 1128 by Instron Co. Ltd. through a cross-head. A photograph of an elevated temperature test of a 2T stiffened panel (02) is shown in Fig. 8. Because of a shortage of width in the environmental chamber, it can be seen that the panel was placed diagonally to it. Also, acoustic emission sensors can be identified by lead wires. Due to such a test piece arrangement in the chamber, Moiré-topography pictures could never be taken at all elevated temperature tests. Instead, those Moiré pictures were taken at room temperature tests.

5. DISCUSSION OF CAI TEST RESULTS

From here on, major discussion will be limited to the results of 2T panels because they are more mechanically interesting. Stress–strain behavior of 2T-01 panel tested at room temperature and 2T-04 panel tested at 180°C is indicated in Figs 9 and 10, respectively. It can be seen clearly that local buckling occurred in an inter-bay

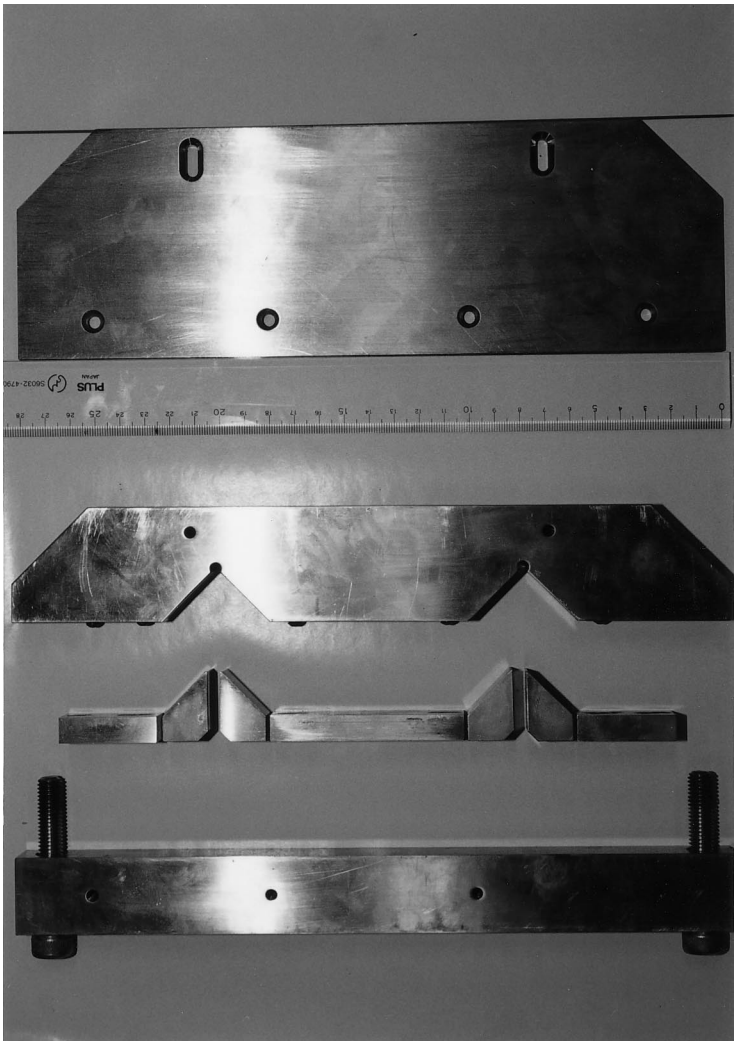

Figure 7. Photograph of loading end fixtures for avoiding high-temperature potting.

between stiffeners at 257 MPa in 2T-01 and that considerable increase in stress–strain relation was observed before the final failure. In other words, substantial postbuckling behavior could be observed in 2T-01. High temperature stress–strain relation of 2T-04 shown in Fig. 10 also describes a considerable post-buckling behavior. In the reported [10] high temperature test (2T-02), a sudden failure after buckling was observed. When this panel was subjected to ultrasonic inspection, several indications of intermediate level were suspected to be a cause of this sort of premature failure behavior. No ultrasonic indications corresponding to fabrication defects were found for other new panels (03-05). A very remarkable feature of CF/PIXA panels bonded by PIXA-M film — that impact delamination was not a trigger of the final failure — will be demonstrated and discussed later.

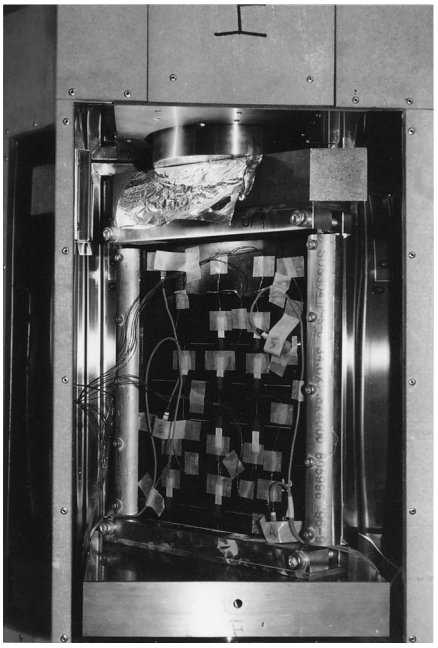

Figure 8. Photograph of high temperature CAI test for 2T panel in chamber.

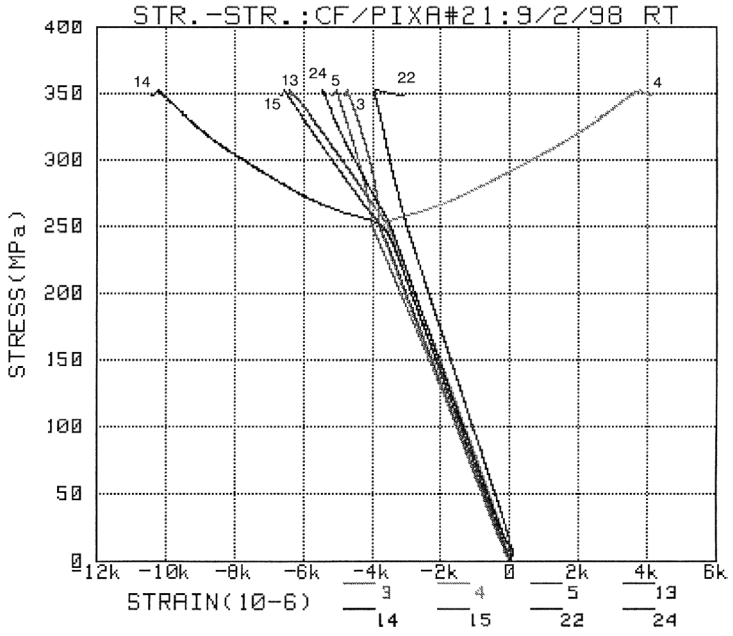

Figure 9. Stress–strain behavior in 2T-01 at room temperature (at 4 J/mm).

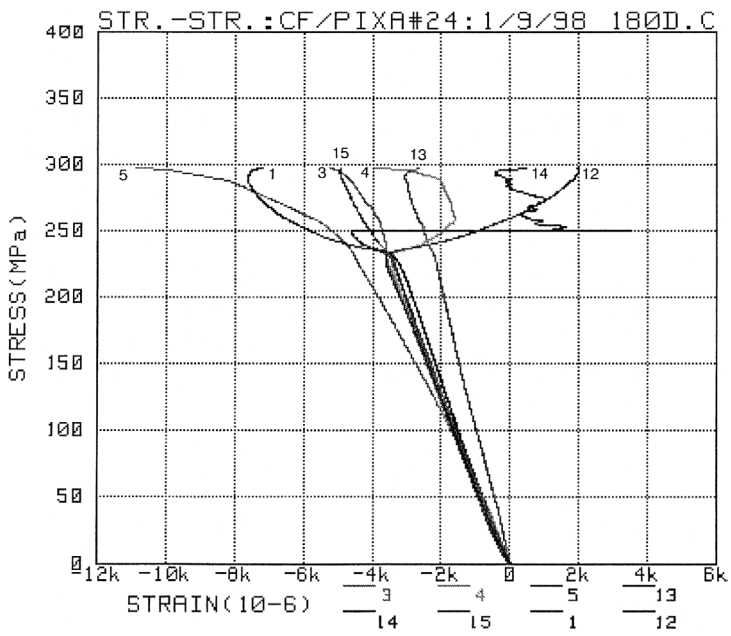

Figure 10. Stress–strain behavior in 2T-04 at 180°C (at 4 J/mm).

Although a presentation of stress–strain behavior of 1T panels is not shown, short comments will be given below. As expected, these 1T panels did not show any post-buckling behavior and failed from material-based compressive instability. Although the strength of 1T-01 at room temperature exhibits a slightly lower value than expected, new panels such as 1T-03 and 04 exhibited quite high CAI strengths indicated below. Again, the quality of the 1T-01 panel affected its strength.

Relationships between normalized impact energy and CAI strengths of stiffened panels at room temperature are shown in Fig. 11 by solid and open circles for CF/PIXA 2T and CF/PIXA 1T, respectively. The previous results for several CF/PEEK stiffened panels are also plotted in this figure for reference, where the legends used are: Solid diamonds for hat stiffened panels fabricated without autoclave [9], solid triangles (FY89) and open squares (FY88) for T-stiffened panels with 4 stringers [8]. It can be understood that better quality panels of the present 2T shows remarkable insensitivity in CAI strength-to-impact energy. In 1T panels, even a reverse relation is observed due to an insufficient quality of 1T-01. From the other aspect, this reverse relation can be regarded as a proof of excellent damage tolerance of these CF/PIXA stiffened panels. A photograph of all the failed 2T panels is shown in Fig. 12 where one remarkable feature of the present experiments — that the impact delamination region was not a trigger of the final failure — can be seen. In all other stiffened panel CAI tests conducted by the authors [8, 9], the final failure was always induced by a transverse delamination penetration between skin and stiffener originating from impact delamination. In the present CF/PIXA panels, they failed in the over-bending deflection mode in post-buckling phase as if delamination

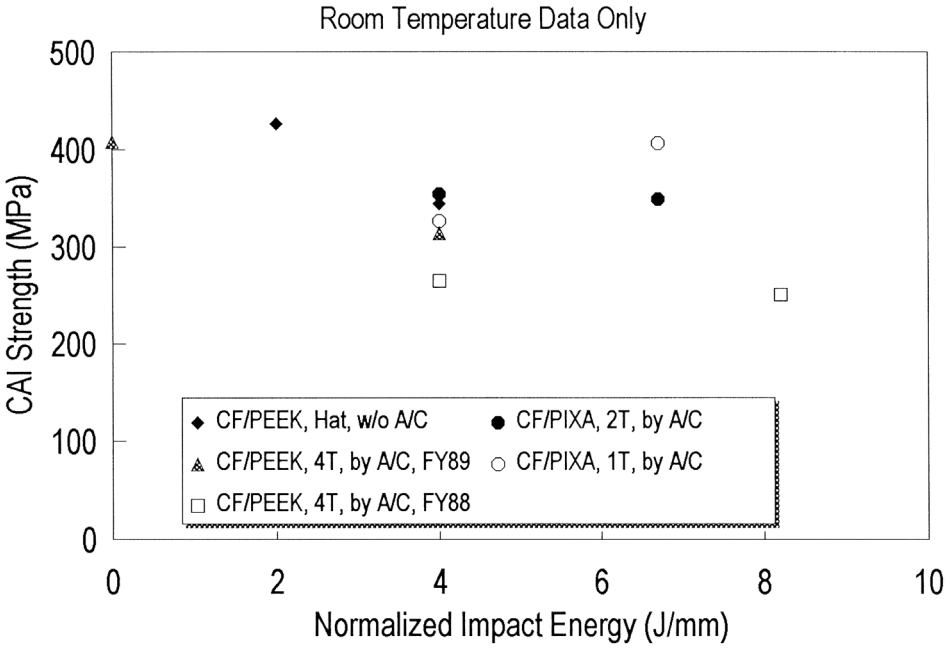

Figure 11. Relationships between normalized impact energy by thickness and stiffened panel CAI strengths at room temperature.

did not exist. Such a pure compression failure mode may contribute to render the numerical predictions simple. This delamination resistance is a superficial reason why CF/PIXA panels exhibited much better CAI strengths than CF/ PEEK panels. The reason for the delamination resistance is still under investigation, although one possible factor of high G_{II} value of fusion bonding surface can be attributed.

Relationships between temperature and CAI strengths for heat-resistant polymer composites are shown in Fig. 13 with the same legends for the present stiffened panels as Fig. 11. Other legend data, CF/PIXA: SACMA, CF/PI-SP: NASA, and CF/BMI: SACMA are results of flat plate CAI strengths identical to those that appeared already in Fig. 1. This figure implies that panel CAI strengths of CF/PIXA are compatible with flat plate behavior. It is also suggested that some panels of insufficient quality exhibited lower CAI strengths. Sufficient post-buckling behavior was observed even at high temperature of 180°C for polymer composite structures if the fabrication process is appropriate. This finding is quite favorable for future HSCT structural design. By summarizing the results in Figs 11, 12 and 13, and Fig. 1, it can be stated that damage tolerance capability of CF/PIXA structure is excellent even at elevated temperatures.

The above finding suggests that the great potential of the CF/PIXA system has been demonstrated as a candidate for HSCT composite structures. It should be noted also that these CAI results provide the basis for an adjustment of actual

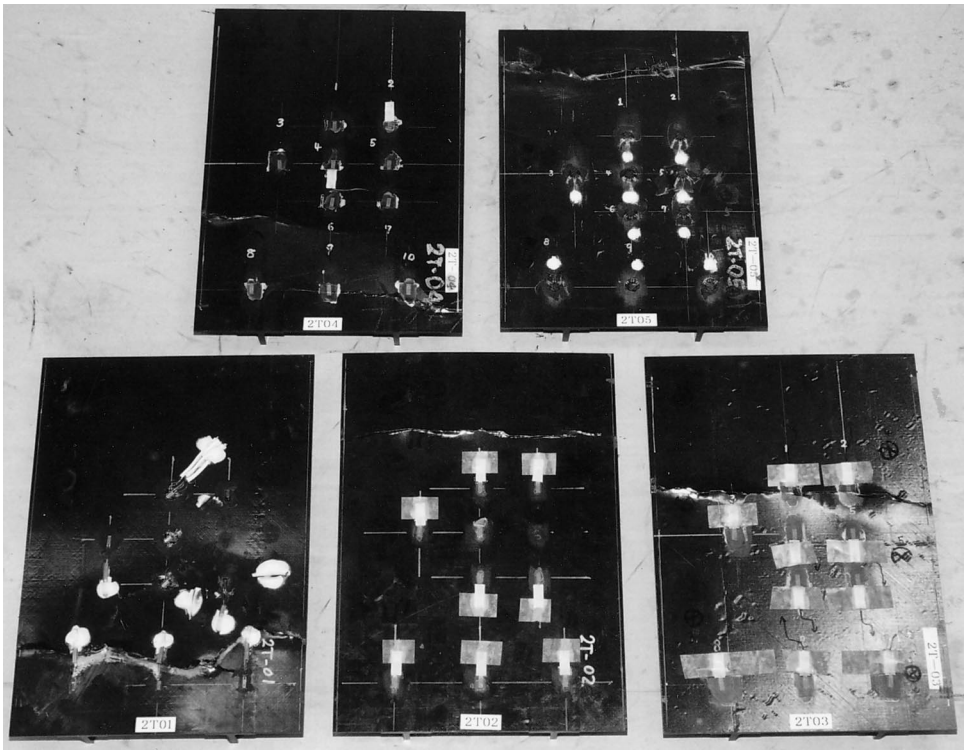

Figure 12. Failed 2T panels with final failure lines independent of impacts: proof of excellent delamination propagation resistance.

allowable stress or strain in a CF/PIXA model wing box test under simulated variable environments which continues now in NAL.

6. COMPARISON OF FEA BUCKLING RESULTS WITH EXPERIMENTS

Numerical calculations using a simple finite element analysis (FEA) were conducted to predict buckling stresses and modes at room and elevated temperatures. The purposes of the analysis are to examine predictability of the simple FEA analysis where interlaminar normal and shear stresses, and delamination were not considered, and to provide a discussion basis as to whether a post-buckling design is possible for high temperature wing box panels or not. Software package of NISA-II was used in the analysis. A quadrilateral laminate shell element of 8 nodes was selected as the base element. Mesh division pattern will be shown in a figure for presenting buckling mode (Fig. 15). Loading and side edges were assumed as fixed and simply supported, respectively. For linear buckling calculations, the simply supported loading edge condition was also adopted for bounding experimental results. Although Ref. [11] employed a combination of fixed and supported boundary conditions, the authors decided that it was not necessary to follow such a condition at least for the

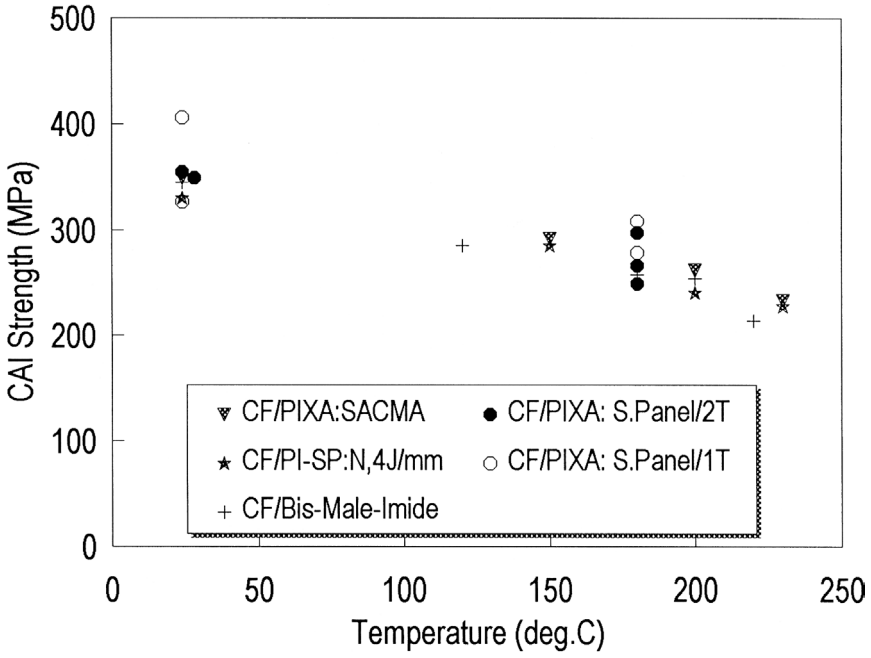

Figure 13. Relationships between temperature and CF/PIXA stiffened panel CAI strengths with reference data of flat plate CAI strengths shown in Fig. 1.

present panels. They incorporated potting and aluminum end plates into the FEA model in their previous work [8], where the panels were wider and shorter. The lowest buckling mode in that case was one half-wave susceptible to loading edge conditions. After a few trials, it was concluded that there is no need to include metallic end fixtures into the model in the present cases. The material properties used from room temperature to 230°C are given in Table 2 and already shown in Fig. 2 (for E_T and G_{LT} only). Although a slight experimental perturbation was observed in actual data for E_L and ν_{LT}, the identical values are assumed for all temperatures. Because no ν_{TT} was available, the authors' standard value was employed here.

It should be noted that precise modeling of panel thickness is quite important for rigorous comparison between experiments and FEA predictions, even if it is a trivial matter in a discipline level. Thickness data of five panels (2T-01 to 05) were measured along two T stiffeners in the compressive direction and FEA model inputs were determined. Figure 14 depicts the measured data and resulting model thickness distribution. Because data for 2T-04 and 2T-05 were similar, one representative model was assumed for these two panels. Note that an intentional shift of 10 mm in the horizontal axis in Fig. 14 is given for 2T-04 and 2T-05 to avoid too much overriding of plots. A tendency that thickness decreases towards panel edges in some cases was caused by the high-pressure fabrication process of this thermoplastic composite system.

Table 2.
Input material properties for CF/PIXA UD lamina for FEA

Temperature (°C)	RT	100	180	230
E_L (GPa)	152.4	152.4	152.4	152.4
E_T (GPa)	8.06	7.65	6.87	5.66
G_{LT} (GPa)	4.69	4.40	3.70	2.80
ν_{LT}	0.344	0.344	0.344	0.344
ν_{TT}	0.5	0.5	0.5	0.5

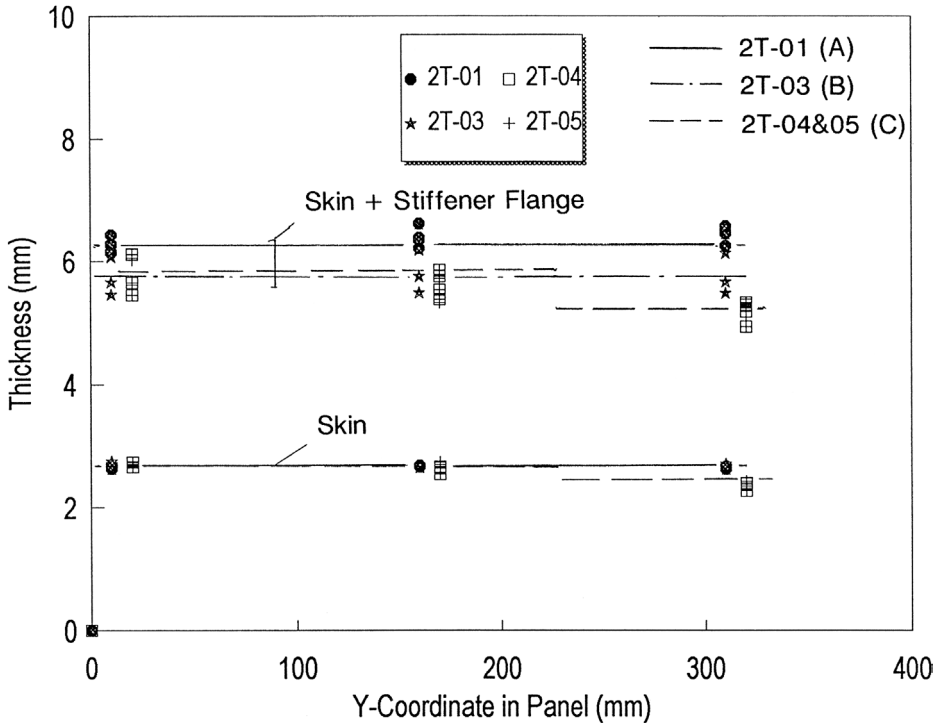

Figure 14. Measured panel thickness distribution and FEA thickness data along longitudinal direction: three model groups of A, B, and C.

At the first phase, linear buckling behavior will be discussed. Calculated buckling mode in out-of-plane deflection contour at room temperature is given in Fig. 15 for 2T-04/05 thickness model. Four half-waves can be identified, where the top region in the plot corresponds to the thinner element portion. An experimental buckling mode taken by the Moiré camera for the objective panel (2T-05) just before failure is shown in Fig. 16 where buckling stress was 228 MPa and no mode transition was observed. Although the lowest half-wave contour is difficult to find in the Moiré picture, an excellent correlation between an experimental mode and FEA prediction can be observed, including slight skewness in the contour shape. This skewness

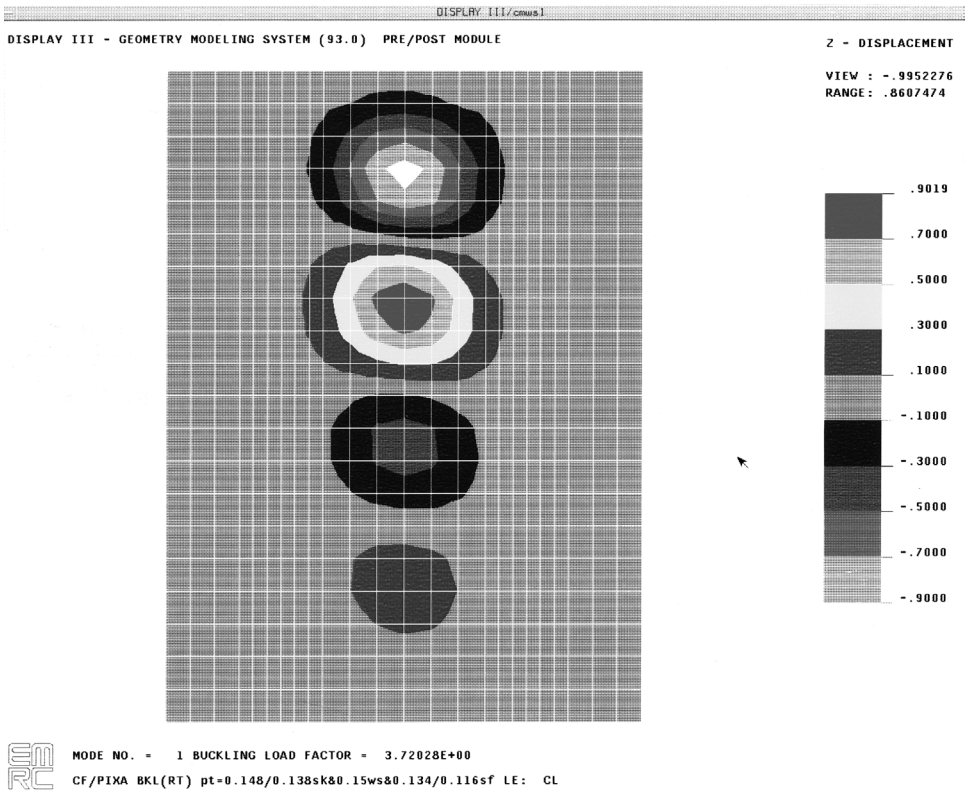

Figure 15. Calculated buckling mode for 2T-05 at RT by NISA-II based on thickness data Group C.

is brought about by local asymmetry in stacking sequence in the skin-attachment flange. Unlike the authors' previous investigations [8, 9], a local buckling on a delaminated area related skin-stiffener separation was not captured through a Moiré picture. This fact leads to one assumption for the present simple modeling without delamination consideration.

Relationships between initial buckling stress and temperature are indicated in Fig. 17 where two cases of loading edge boundary conditions, clamped and simply supported, and three thickness data groups (A, B and C) are adopted in FEA predictions. If we look at experimental initial buckling stress of 2T-01 and 2T-03, they are bounded by each set of two curves of the two boundary conditions for thickness data A and B, respectively. A similar situation happens with buckling stresses of 2T-04 and 05. A tendency that two FEA curves become open based on the thinner edge model (C) is recognized. If we consider the magnified vertical axis in Fig. 17, agreement between experiments and FEA predictions can be regarded as sufficiently good. This figure suggests a practical conclusion that only a slight reduction of initial buckling stress is observed at high temperature. In other words, it is implied that the post-buckling region at high temperature should be limited if the final strength of the panel is low.

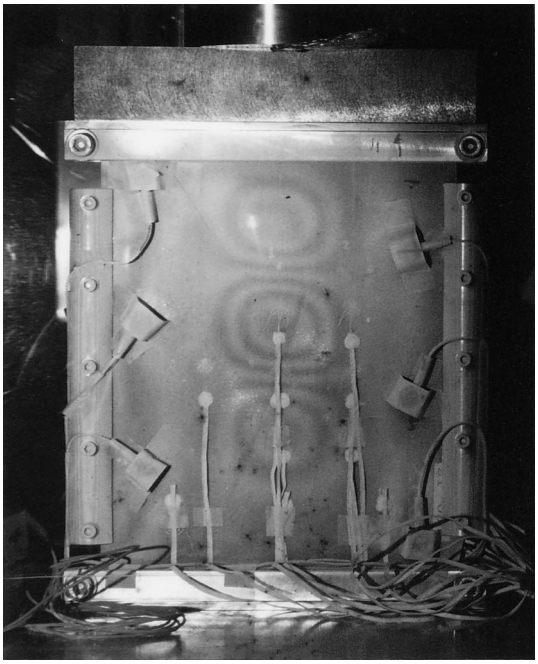

Figure 16. Experimental buckling pattern for 2T-05 taken by Moiré-camera.

In order to clarify such implication and to provide a discussion basis for establishment of post-buckling design philosophy for stiffened panels at high temperature, geometrical nonlinear post-buckling analysis was conducted for the same FEA model. Introduction of appropriate initial imperfection is a key factor for such a calculation as the authors' previous work [12]. According to measurements of waviness of the panel and several trial calculations, it was determined that a sinusoidal initial imperfection function of $1/100$ mm amplitude and of one period between two loading edges and of one half-period between stiffeners is sufficient and appropriate. By applying such an initial imperfection, geometrical non-linear post-buckling analysis is possible in NISA-II software. A tolerance of $2/1000$ as a relative vector norm change was used for convergence check in each loading step. Displacement controlled analysis at the loading edge, i.e. a situation that all nodes along the compression surface have the identical assigned displacement, was conducted to simulate the actual flat compression.

An experimental-numerical comparison for the out-of-plane displacement change for 2T-01 at room temperature is shown in Fig. 18. The continuous curves indicate outputs of deflection pick-ups and solid circles and triangles are calculated values in which a location shift of 25 mm in the loading direction is applied so as to coincide the experimental and numerical peaks in the deflection contour. Note that an experimental deflection shift of 0.14 mm at null stress is assumed zero deflection in plotting the calculation. Correlation between experiments and FEA prediction is fairly good under the two adjustments stated above. It can be concluded that

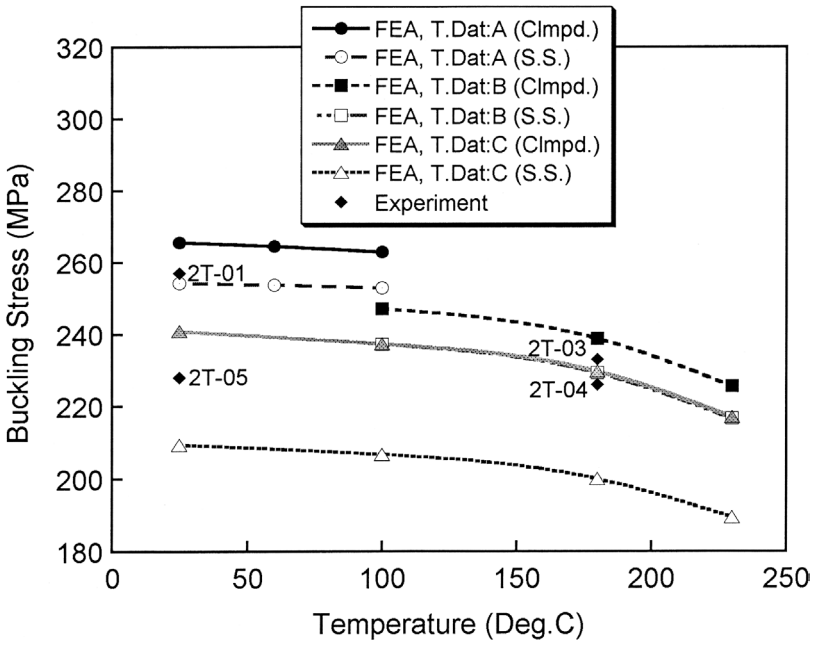

Figure 17. Relationships between initial buckling stress and temperature: comparison of experimental results with numerical predictions of two loading edge conditions based on three thickness data groups.

the present post-buckling analysis describes the experimental behavior sufficiently well. An experimental-numerical comparison for stress–strain relations for the same panel is shown in Fig. 19. Experimental strain plots are identical to Fig. 9 and legend conventions are the same as Fig. 18. Strain values at the closest output locations to the gages were calculated through in-plane stress data. The extent of correlation between experiments and predictions in strain becomes slightly worse than in the deflection case.

Based on the above preparation, it is possible to predict the final strength of the panel if we admit the following simplified assumptions in the present calculation:

1. No interlaminar stresses govern the final strength.
2. Delamination does not affect the strength as the experiments indicated.
3. Final failure occurs when the lamina stress in any part of the panel reaches the prescribed failure criterion.

Here, the maximum stress criterion was employed for the sake of simplicity. According to some trial calculations, it can be found that compressive stress in the 0° lamina nearest to the skin surface or to attachment flange surface is quite predominant among all stress components due to buckling deformation. By tracing this stress component in each loading step and by an interpolation, we can determine the overall final load and failure stress. Note that the average value in the lamina in a bending state, i.e. a central surface value of lamina, is

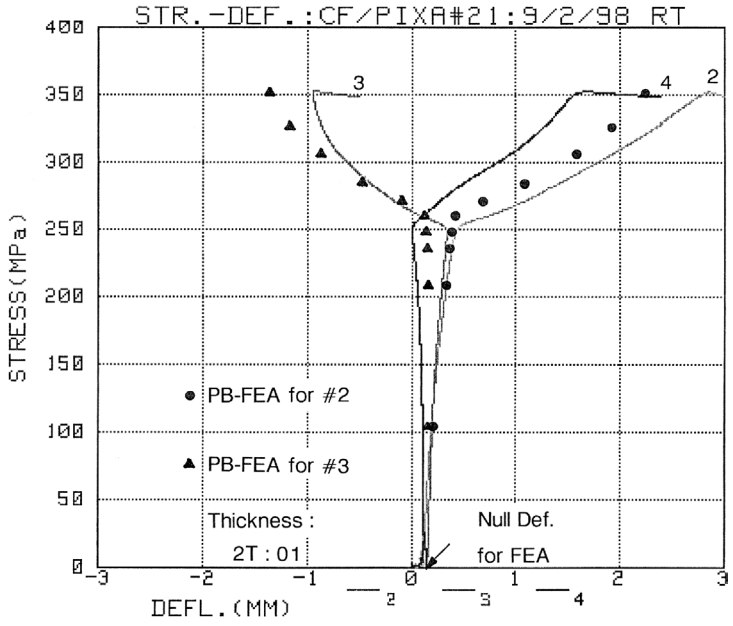

Figure 18. Comparison between FEA predictions and experiments in stress/out-of-plane deflection relations for 2T-01 at room temperature.

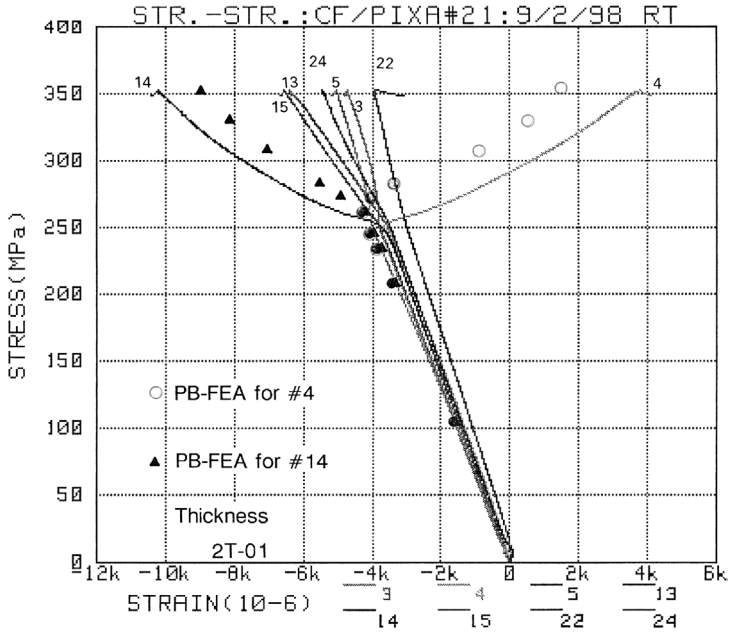

Figure 19. Comparison between FEA predictions and experiments in stress–strain relations for 2T-01 at room temperature.

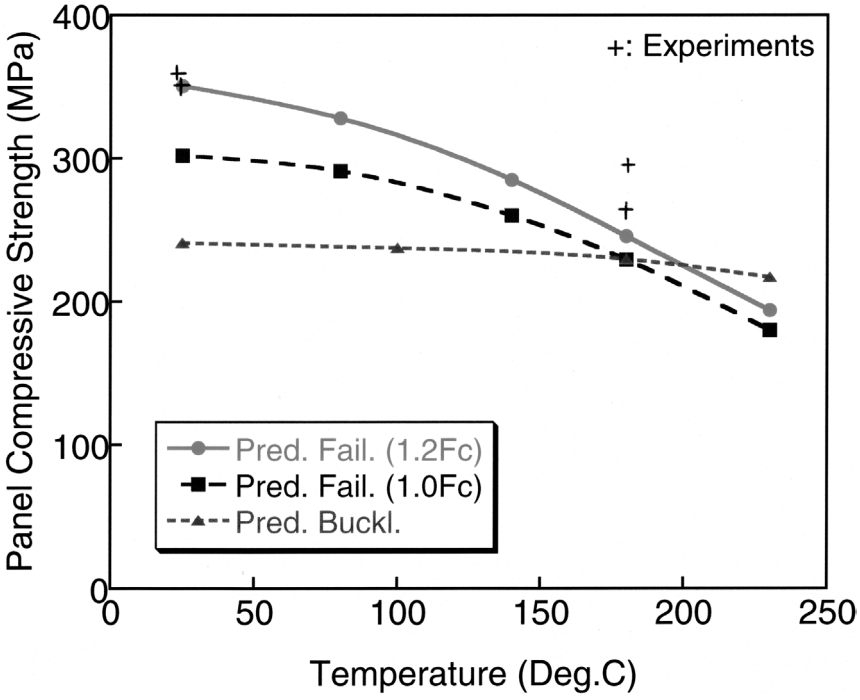

Figure 20. Comparison between final failure strength predictions by post-buckling FEA based on in-plane lamina stress and experimental strengths at elevated temperatures.

adopted here. Figure 20 depicts the results of such failure predictions. If we use the results of UD compressive strengths (F_c) in Fig. 3 straightforwardly, the curve marked with filled square is obtained. If we assume an adjustment factor of 1.2 to allow for the difference in thickness of lamina in the panel (1 ply) and an ASTM-D3410/A specimen (16 plies), the curve marked by the filled circle in Fig. 20 is obtained. There is no rational foundation for the factor of 1.2 and it is a rather intuitive value. It can be seen that experimental strengths coincide with predictions based on the $1.2F_c$ curve at room temperature, and that experimental results become slightly higher at 180°C. The present numerical calculation does not predict the final strength perfectly. In other words, if we rely on calculations, we do not see considerable post-buckling behavior at high temperature observed in the experiments. One possible reason for this small discrepancy might be the thermal residual stress being reduced at elevated temperature. So, a simple estimation of thermal residual stress in each lamina was conducted based on the in-plane state, temperature dependent material properties and stress-free temperature of 280°C. The results yield −30.9 MPa at room temperature and −11.9 MPa at 180°C in the longitudinal direction of the 0° lamina. If we compare these results with the F_c about 1.0 GPa, a 2% improvement in prediction (upward) will be achieved in the framework of the present simple calculation. Although this consideration of residual stress moves things in a better direction, it does not provide a perfect agreement. In

order to obtain such a full description of the behavior by numerical calculation, much more sophisticated analysis will be needed. However, a consideration that almost no post-buckling behavior will be expected at 230°C can be reached even by the present primitive modeling. This sort of information seems to be valuable for establishing design concept of HSCT composite structures.

7. CONCLUSIONS

CAI strengths of stiffened panels of CF/PIXA were obtained at room temperature and elevated temperature of 180°C. The following findings are obtained through the experiments and corresponding numerical analysis using simple FEA model for initial buckling prediction and non-linear post-buckling behavior without a consideration of the delamination.

1. CF/PIXA stiffened panels demonstrate their excellent impact resistance at ambient temperature. It is even better than CF/PEEK and one possible reason for such a good resistance may be high fracture toughness provided by Regulus PIXA-M fusion-bonding film used between skin and attachment flange.
2. A comparison of all structural CAI data of various materials indicates that damage tolerance properties of CF/PIXA are quite excellent even at elevated temperature if the structure is well fabricated.
3. Delaminated regions by impact were not triggers of the final failure in the present stiffened panel tests owing to excellent delamination evolution resistance of the present fusion bonding.
4. A stiffened panel with two T stringers tested at room temperature exhibited substantial post-buckling behavior. The panel tested at high temperature also showed enough post-buckling behavior if fusion bonding is well accomplished.
5. CAI results of stiffened panels are highly consistent with flat plate CAI results of the same material done in SACMA method.
6. Numerical calculations by FEA can predict well for linear buckling stresses, post-buckling deflection and post-buckling stress–strain behavior. For prediction of the final strength, more sophisticated analysis will be required.
7. Special end clamping devices were developed and proven to be effective in high temperature CAI tests of stiffened panels. Ordinary AE sensors worked so far as the tested temperature (180°C).
8. There is still some scatter in CAI values for 1T and 2T panels.
9. Obtained results are directly used for a determination of allowable strain or stress in a model wing box test of CF/PIXA conducted in NAL under variable environments.

Acknowledgements

This work is sponsored by a special research program for HSCT composite structure in NAL funded from STA of Japanese Government. The authors wish to express their gratitude to related people in Fuji Heavy Industries for supplying CF/PIXA test panels of such high quality. They are also thankful to two students: Mr. Eugine K. G. Lim of RMIT for his support in CAI tests and Mr. H. Kumazawa of Tokyo University for his calculation of thermal residual stresses.

REFERENCES

1. H. Nakamura, Y. Toi and N. Ando, Composite materials and structure development in FHI for high-speed civil transport, in: *Proc. 1996 World Aviation Congress*, Los Angeles, CA, USA, SAE-965582 (1996).
2. T. Ishikawa, M. Matsushima, Y. Hayashi and H. Nakamura, Strengths of heat resistant thermoplastic composites (IM-7/PIXA) for future high speed civil transport, in: *Proc. 5th Jpn. Int SAMPE Symp.*, Tokyo, Japan, pp. 1137–1142 (1997).
3. T. Ishikawa, M. Matsushima, S. Esaki, K. Matsui and M. Sunakawa, CAI properties of heat resistant thermoplastic composites (CF/PI-SP) at room and elevated temperatures, in: *Proc. Ann. Mtg. Jap. Soc. Compos. Mater.*, Tokyo, Japan, pp. 53–54 (1996) (in Japanese).
4. T. Shimokawa, Y. Hamaguchi, Y. Kakuta, H. Katoh, T. Sanda, H. Mizuno and Y. Toi, Effect of isothermal aging on strength of high-temperature composite materials for SST structures, *J. Compos. Mater.* **33**, 1104–1108 (1999).
5. SACMA, *Recommended Test Method for CAI Properties*, SRM2-88 (1988).
6. M. Noda, Y. Ito and S. Miyamoto, Mechanical properties of polymer composites based on toughened bis-maleimide, in: *Proc. 30th Aircraft Sympos.*, Japan Society of Aeronautical and Space Sciences, Tsukuba, Japan, pp. 498–501 (1992) (in Japanese).
7. T. Ishikawa, M. Matsushima and Y. Hayashi, Comparison and discussion about compression after impact (CAI) properties obtained by SACMA and NASA methods, in: *Proc. 8th US/Japanese Conf. Compos. Mater.*, Baltimore, MD, USA, G. M. Newaz and R. F. Gibson (Eds), pp. 476–485. American Society for Composites (1998).
8. T. Ishikawa, M. Matsushima and Y. Hayashi, Improved correlation of predicted and experimental initial buckling stresses of composite stiffened panels, *Compos. Struct.* **26**, 25–38 (1993).
9. T. Ishikawa and M. Matsushima, Compression after impact (CAI) properties of heat stiffened CF/PPEK panels fabricated through a route without autoclave, in: *Proc. 11th Int Conf. Compos. Mater.*, Melbourne, Australia, Vol. II, L. M. Scott (Ed.), pp. 1–9 (1997).
10. T. Ishikawa, M. Matsushima, E. K. G. Lim, Y. Hayashi and M. L. Scott, Compression after impact properties of flat and stiffened CF/PIXA panels for HSCT structure, in: *Proc. 13th Ann. Tech. Conf. Compos. Mater.*, Baltimore, MD, USA, A. J. Vizzini (Ed.), pp. 1776–1786. American Society for Composites (1998).
11. J. H. Starnes, Jr., N. F. Knight, Jr. and M. Rouse, Post-buckling behavior of selected flat stiffened graphite-epoxy panels loaded in compression, *AIAA Journal* **23**, 1236–1246 (1985).
12. T. Ishikawa, M. Matsushima and Y. Hayashi, Comparison of numerical analysis of linear and nonlinear postbuckling behavior of CFRP T-stiffeners with experimental results, *Adv. Composite Mater.* **7**, 263–283 (1998).